Crystal-field excitations in $PrAl_3$ and $NdAl_3$ at ambient and elevated pressure

2003 J. Phys.: Condens. Matter 15 3257

(http://iopscience.iop.org/0953-8984/15/19/325)

INSTITUTE OF PHYSICS PUBLISHING JOURNAL OF PHYSICS: CONDENSED MATTER

J. Phys.: Condens. Matter **15** (2003) 3257–3266 PII: S0953-8984(03)59053-1

Crystal-field excitations in $PrAl_3$ and $NdAl_3$ at ambient and elevated pressure

Th Strässle[1,4,5], M Diviš[2], J Rusz[2], S Janssen[1], F Juranyi[1], R Sadykov[3] and A Furrer[1]

[1] Laboratory for Neutron Scattering, ETH Zürich and Paul Scherrer Institut, 5232 Villigen PSI, Switzerland
[2] Department of Electronic Structures, Charles University, Ke Karlova 5, 121 16 Prague 2, The Czech Republic
[3] Vereshchagin High-Pressure Physics Institute RAS, 142190 Troitsk, Moscow region, Russia

E-mail: thierry.strassle@pmc.jussieu.fr

Received 3 February 2003
Published 6 May 2003
Online at stacks.iop.org/JPhysCM/15/3257

Abstract

The crystal fields (CFs) of the binary rare-earth compounds $PrAl_3$ and $NdAl_3$ have been examined at ambient pressure by means of inelastic neutron scattering. The CF of the latter compound has also been measured under hydrostatic pressure ($p = 0.84$ GPa). The observed substantial changes of the CF under pressure are discussed within the framework of first-principles density functional theory calculations.

1. Introduction

For most rare-earth compounds the magnetic properties are decisively governed by the crystal-field (CF) interaction. Inelastic neutron scattering (INS) has proved to be the most versatile experimental tool for determining the CF interaction in metallic systems. On the other hand, there is a lack of theoretical tools which are able to predict the CF interaction with sufficient precision. The situation may be more favourable with regard to extrapolation schemes which predict the CF interaction for isostructural compounds upon altering the lattice parameters by rare-earth substitution or pressure. This issue is addressed in the present work for the light rare-earth compounds $PrAl_3$ and $NdAl_3$.

$PrAl_3$ and $NdAl_3$ crystallize in the hexagonal structure type Ni_3Sn (space group $P6_3/mmc$). The low magnetic ordering temperature of $NdAl_3$ ($T_N = 4.1$ K) as well as the absence of magnetic ordering in $PrAl_3$ makes these compounds ideal candidates for precise CF studies, since broadening of the CF transitions due to magnetic dispersion effects is expected

[4] Author to whom any correspondence should be addressed.
[5] Present address: Physique des Milieux Condensés, Université Pierre et Marie Curie B77, 4 Place Jussieu, 75252 Paris, France.

to be small. Moreover, the hexagonal structure allows a change of the lattice parameter ratio c/a under hydrostatic pressure p. We have performed INS experiments for $PrAl_3$ ($p = 0$) and $NdAl_3$ ($p = 0$ and 0.84 GPa) which allowed for an unambiguous determination of the CF parameters. Our data clarify earlier INS studies of the CF in these compounds which resulted either in different possible sets of CF parameters for $PrAl_3$ [1–4] or uncertainties about the CF ground state in $NdAl_3$ [5]. The CF parameters obtained in the present work are examined with regard to extrapolation schemes based on the extended point-charge model (PCM) and first principles density functional theory (DFT).

2. Experimental details

Details of the sample preparation have been published elsewhere [6]. Both samples have been characterized by x-ray diffraction. The $PrAl_3$ sample did not show any impurity phases, whereas for the $NdAl_3$ sample tiny amounts (<1%) of $NdAl_2$ and Nd_3Al_{11} have been found. The lattice parameters at room temperature correspond to published values [8]. The only free atomic position parameter of Al is found $x_{Al} = 0.858(1)$ for both compounds. The INS experiments have been carried out on the time-of-flight (TOF) spectrometer FOCUS at the SINQ spallation neutron source of PSI in Villigen, Switzerland. The incoming neutron energy was chosen to be 18.7 meV. By inelastic time focusing the minimum of the resolution function was set to a neutron energy loss of 10 meV. For the measurements at ambient pressure the polycrystalline powder samples were placed in aluminium cans of 10 mm diameter and were cooled in a standard ILL cryostat. The measurements on $NdAl_3$ under pressure were carried out in a pressure cell designed for FOCUS. The axial symmetric cell made of hardened aluminium allows measurements up to 1 GPa pressure with minimal loss in intensity due to absorption of the neutrons. The cell of 70 mm outer diameter contains an inner steel core of 1.5 mm thickness and 7.2 mm inner diameter. The total accessible sample volume in the cell amounts to about 1600 mm^3. Pressure was determined at base temperature by the shift in the lattice parameter of NaCl [7] added to the sample. For this purpose the lattice parameters of the sample and of NaCl were measured on the powder diffractometer HRPT at SINQ in the pressure cell in the very same sample environment prior to the INS measurements.

The measurements of the magnetic susceptibility were carried out on a Quantum Design PPMS system. A clamp cell made of non-magnetic Cu/Be alloy was used, allowing pressures up to 1 GPa. Within the cell the sample was placed in a very thin capsule made of lead and filled with Fluorinert FC-77. The superconducting transition temperature of the lead was used to measure the pressure [9].

3. Results and data analysis

The inelastic neutron spectra of $PrAl_3$ are shown in figure 1 for ambient pressure. The strong transition at 4.5 meV can readily be ascribed to a transition from the ground state. Note that this transition dominates over the incoherent elastic scattering. All additional intensity in the $T = 65$ K spectrum is attributed to transitions from excited CF levels. For the hexagonal point group D_{3h} of the rare-earth site, the CF can be described by the Hamiltonian [13]

$$\hat{\mathcal{H}}_{CF} = B_2^0\hat{O}_2^0 + B_4^0\hat{O}_4^0 + B_6^0\hat{O}_6^0 + B_6^6\hat{O}_6^6 \tag{1}$$

with B_n^m and $\hat{O}_n^m$ being the CF parameters and Stevens operators, respectively. With the energy levels and neutron transition matrix elements resulting from diagonalization of equation (1) the spectra have been analysed by a least-squares procedure for both temperatures simultaneously. The best-fit parameters are listed in table 1. The resulting CF level scheme is shown in figure 2.

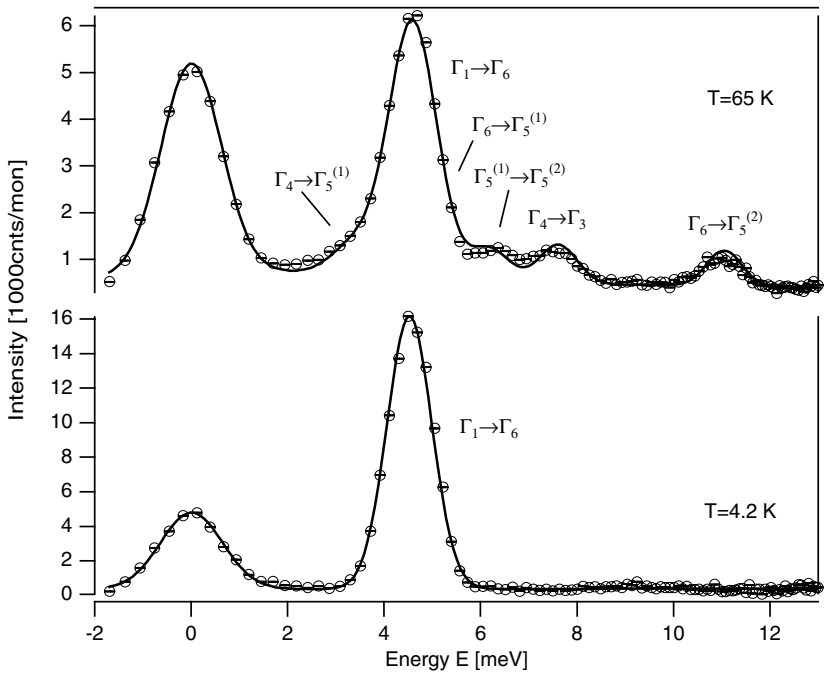

Figure 1. Observed inelastic neutron spectra for $PrAl_3$ at ambient pressure together with the calculated spectra using the best-fit parameters listed in table 1 (note the different scalings).

Table 1. Lattice parameters and best-fit parameters for the CF in $PrAl_3$ and $NdAl_3$ (Stevens notation, all parameters in millielectronvolts; lattice parameters of $PrAl_3$ from x-ray diffraction at room temperature, $NdAl_3$ from neutron diffraction at 10 K). Note that the sign of B_6^6 remains undetermined in D_{3h} point symmetry [13].

	p (GPa)	a (Å)	c (Å)	B_2^0	$B_4^0 \times 10^2$	$B_6^0 \times 10^3$	$B_6^6 \times 10^2$
$PrAl_3$	0	6.5121(4)	4.6038(3)	0.203(9)	−0.166(10)	0.114(3)	±0.151(6)
$NdAl_3$	0	6.455(1)	4.589(4)	0.095(2)	−0.061(5)	−0.071(1)	±0.082(1)
$NdAl_3$	0.84(5)	6.432(4)	4.564(9)	0.105(8)	−0.056(11)	−0.078(2)	±0.087(5)

The CF parameters determined in this work are in accordance with values published earlier by Alekseev *et al* [2] on the basis of less resolved thermal TOF INS spectra.

The spectrum at 10 K found for $NdAl_3$ is characterized by three well resolved CF transitions (figure 3). A least-squares fitting of the spectrum resulted in the parameters listed in table 1. The values found are close to the ones published by Alekseev *et al* [5], which to our knowledge constitute the only CF set determined from INS measurements. The corresponding level scheme is depicted in figure 2. Additional measurements carried out at higher experimental resolution did not reveal any further information about the $\Gamma_9^1 \leftrightarrow \Gamma_8^1$ transition as it overlaps with the elastic and quasielastic line. In contrast to the CF of Alekseev the ground state is not found to be a Γ_8 but a Γ_9 state. Hence our set results in a somewhat larger saturated moment of the Nd^{3+} ion than Alekseev's ($\mu_{Nd} = 2.19\ \mu_B$ as opposed to $\mu_{Nd} = 2.07\ \mu_B$). Both sets result in an easy magnetic axis perpendicular to the c-axis.

The spectra of $NdAl_3$ in the pressure cell at ambient pressure and at $p = 0.84(5)$ GPa are presented in figure 4. The measurement at ambient pressure corresponds well to the

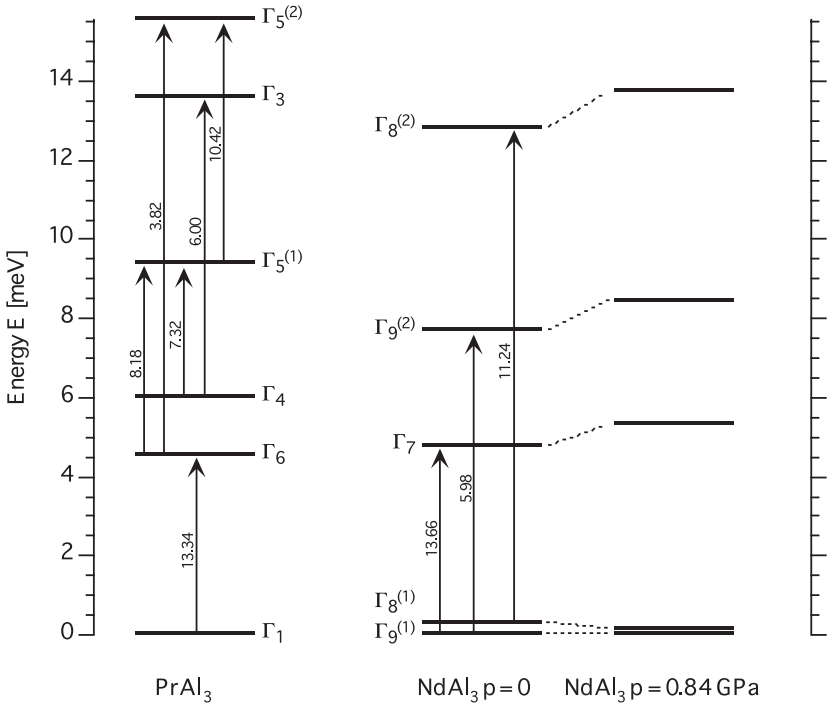

Figure 2. Energy level schemes for $NdAl_3$ and $PrAl_3$ (the arrows depict observed transitions; the numbers denote absolute squares of the neutron transition matrix elements; the CF parameters are taken from table 1).

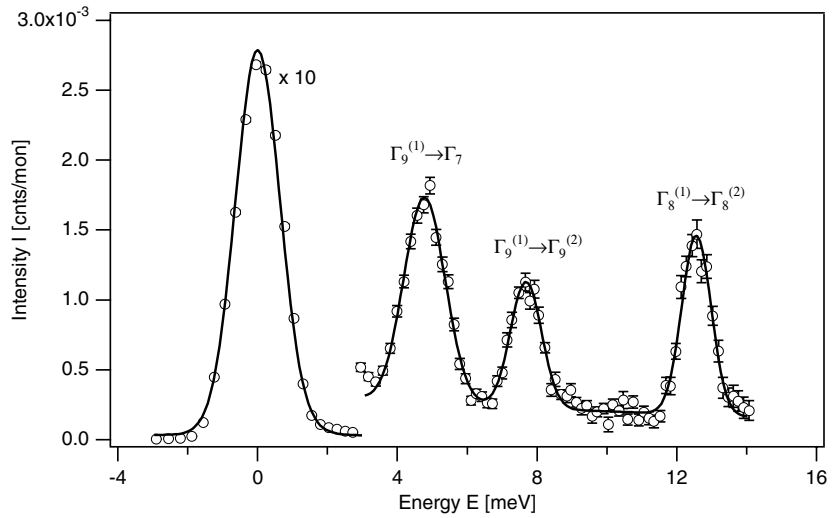

Figure 3. Observed inelastic neutron spectra for $NdAl_3$ at ambient pressure ($T = 10$ K) together with the calculated spectra using the best-fit parameters listed in table 1.

measurement made in the aluminium can except for an effective loss in intensity by a factor of six due to the absorption by the cell (for about the same sample volume). Pressure leads to an overall shift of the spectrum to higher energies without any principally new features.

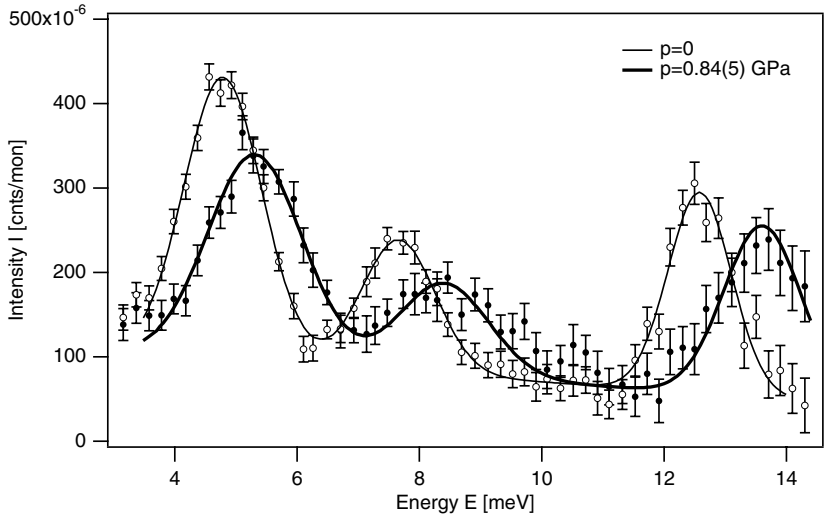

Figure 4. INS spectra for $NdAl_3$ at ambient pressure (in the pressure cell) and at $p = 0.84(5)$ GPa ($T = 10$ K). The solid curves denote calculations based on the best-fit parameters listed in table 1.

The peaks for $p > 0$ are found to be broader than at $p = 0$ as a consequence of pressure distribution. Starting from the CF parameters of $NdAl_3$ at ambient pressure the corresponding parameters at $p > 0$ are readily fitted. Table 1 lists the best-fit parameters of the CF together with the lattice parameters at $p = 0$ and 0.84 GPa. Under pressure all parameters increase in magnitude with the exception of B_4^0 (which has the largest experimental uncertainty). B_6^0 dominates the splitting scheme and increases by as much as 10%. Note that within the accuracy of the neutron diffraction data taken at $p > 0$ no change in the atomic position x_{Al} of the Al ion could be observed. In the following it was thus kept fixed to the value at ambient pressure ($x_{\mathrm{Al}} = 0.858(1)$).

In order to rule out any anomalous pressure dependence of the ordering temperature T_N, we have carried out additional DC magnetization measurements under pressure, which resulted in $\mathrm{d}T_N/\mathrm{d}p = 0.51(6)$ K GPa^{-1} (figure 5). Therefore, the INS measurement at $p = 0.84$ GPa is taken well within the paramagnetic state and the pressure-induced change in the CF must be addressed due to changes in the structure and in the electronic properties and not due to a change in the magnetism of the system. With the CF parameters for ambient pressure and $p = 0.84$ GPa at hand, we may further examine the effect of the changed CF on the ordering temperature T_N. With a simple mean-field model we may obtain the molecular parameter λ to account for the observed T_N at ambient pressure. Substituting this value back into a mean-field calculation using the CF parameters for $p = 0.84$, we find T_N to change as $\mathrm{d}T_N/\mathrm{d}p \sim 0.35$ K GPa^{-1}. It should be noted that pressure is strongly expected to change the strength of exchange (i.e. λ) too. The above simple calculation is thus not meant to give a quantitative explanation for the observed $\mathrm{d}T_N/\mathrm{d}p$, but rather demonstrates that apart from $\lambda(p)$, the altered CF(p) has a large influence on T_N in $NdAl_3$.

4. Discussion

4.1. Extended point-charge model of the CF

Within a simple picture, the CF of $NdAl_3$ and $PrAl_3$ may be discussed in terms of the PCM [10]

$$B_n^m = a_n^m \langle r^n \rangle \chi_n \gamma_n^m \tag{2}$$

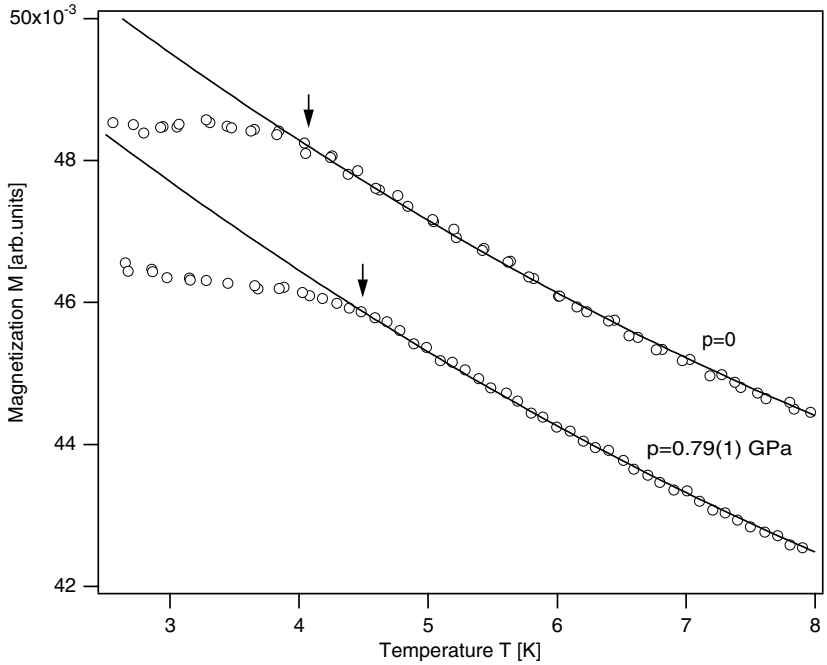

Figure 5. Pressure effect on the Néel temperature of $NdAl_3$ determined by measurement of the DC magnetization (values in arbitrary units including contributions of the pressure cell and pressure calibrant). Arrows denote the ordering temperature where the magnetization curves deviate from the paramagnetic behaviour (solid line).

with reduced CF parameters a_n^m reflecting the charge distribution independent of geometry and type of rare earth, $\langle r^n \rangle$ the nth radial moment of the 4f electron, χ_n the Stevens coefficients and geometric coordination factors γ_n^m calculated by the PCM. Morrison [10] has introduced an extension of the original PCM, which corrects the free Hartree–Fock 4f radial moments $\langle r^n \rangle \rightarrow \langle r^n \rangle / \tau^n$ for the situation of ions embedded in solids and which takes into account the shielding due to the outer $5s^2$ and $5p^6$ shells of the rare-earth ion by scaling $B_n^m \rightarrow (1-\sigma_n) B_n^m$. τ and σ_n are phenomenological parameters of the rare-earth ion tabulated in [10]. Even with these extensions the PCM generally fails to predict the parameters quantitatively for metallic compounds. However, it has been proven to be helpful in order to account for general tendencies and dependences of the CF upon changes of the structure or substitutions of ions [12]. As shown below the extended PCM allows us to estimate the pressure dependence of the CF parameters in $NdAl_3$ quite accurately in a straightforward, simple manner.

Table 2 lists the values a_n^m of $NdAl_3$ and $PrAl_3$ for ambient pressure as obtained by the extended PCM with the radial moments $\langle r_n \rangle$ taken from [11]. The geometric coordination factors γ_n^m are calculated from the two closest shells of Al neighbours (six Al, $d_{Nd} \sim 3.151$ Å; six Al, $d_{Nd} \sim 3.240$ Å) and rare-earth neighbours (six R, $d_{Nd} \sim 4.376$ Å; two R, $d_{Nd} \sim 4.589$ Å) [12]. X-ray determined lattice parameters at room temperature were used[6]. The reduced CF parameters are found to be very close to each other with the exception of a_2^0 which results from the obvious weakness of the PCM only considering a small neighbourhood of ions. The close match of the reduced CF parameters points to a similar charge distribution in $PrAl_3$ and $NdAl_3$. With the above geometric factors γ_n^m the CF may now be parametrized

[6] $NdAl_3$: $a = 6.4710(1)$ Å, $c = 4.6005(4)$ Å.

Table 2. Reduced CF parameters of $NdAl_3$ and $PrAl_3$ at ambient pressure as derived with equation (2) from the experimentally observed CF parameters B_n^m of table 1 (all values in (10^4 meVÅ)). Similar values a_n^m are found for $NdAl_3$ and $PrAl_3$.

	a_2^0	a_4^0	a_6^0	a_6^6
$PrAl_3$	0.63(3)	−1.58(9)	−1.68(4)	±2.33(9)
$NdAl_3$	1.00(2)	−1.75(14)	−1.89(3)	±2.28(3)

Table 3. Experimentally observed (exp.) and calculated CF parameters from the extended PCM and from density-functional calculations (DFT) (all values in millielectronvolts, Stevens notation).

	p (GPa)	from	B_2^0	$B_4^0 \times 10^2$	$B_6^0 \times 10^3$	$B_6^6 \times 10^2$
$PrAl_3$	0	Exp.	0.203(9)	−0.166(10)	0.114(3)	0.151(6)
		DFT	0.130	−0.063	0.179	0.239
$NdAl_3$	0	Exp.	0.095(2)	−0.061(5)	−0.071(1)	0.082(1)
		PCM	(−0.055)	−0.095	−0.081	0.082
		DFT	0.052	−0.006	−0.085	0.114
	0.84	Exp.	0.105(8)	−0.056(11)	−0.078(2)	0.087(5)
		PCM	(−0.056)	−0.099	0.083	0.084
		DFT	0.052	−0.009	−0.088	0.117

to reproduce the observed CF parameters at ambient pressure. One obtains for the effective charge of the Al ion $q_{Al} \approx +1.64e$ as the only fitting parameter ($q_{Nd} \equiv +3e$ fixed; B_2^0 excluded from fit). The resulting CF parameters are listed in table 3.

The effect of pressure on the CF due to the geometrical changes may now be roughly estimated by equation (2) with altered γ_n^m corresponding to the lattice parameters at $p > 0$ and with q_{Al} kept fixed to the above value. The resulting parameters are given in table 3. With relative increases of ∼2% (B_4^0: ∼4%), the model underestimates the effect of pressure. Note that the model in this form only accounts for changes in the geometry, but not in the electronic structure. In fact, at first glance, pressure is expected to decrease the density of states at the Fermi level resulting in less screening due to the conduction electrons. Consequently, the CF splitting should tend to become larger for $p > 0$ on account of the changed electronic properties as experimentally observed.

4.2. First principles density functional theory of the CF

In order to obtain additional information about the relation between the electronic structure, the ground-state charge density and the CF in the RAl_3 compounds, we have also calculated the CF from first principles using the DFT. Within this method the electronic structure and the corresponding distribution of the ground-state charge density is obtained using the full potential linearized augmented plane wave method (LAPW) implemented in the latest version of the WIEN97 code [14]. We have applied both the local spin density approximation (LSDA) and the generalized gradient approximation (GGA) [15] for the treatment of the exchange and correlation effects. The band structure and the related charge density were calculated for the experimentally determined structural parameters a, c and $x_{Al} = 0.858$ for both compounds. The atomic forces calculated at the experimental positions of the atoms were quite small and thus the structure must be close to the theoretical equilibrium. This fact also holds for the case of $NdAl_3$ under pressure for which x_{Al} could not be determined experimentally. The GGA calculations provided some smaller forces at the Al position than obtained by the LSDA

calculations. One may thus conclude that GGA yields the best theoretical description of the crystal charge density currently available for the RAl_3 compounds. Consequently, we calculated the CF parameters from the ground-state charge density obtained by the GGA calculations. To simulate the localized 4f states we switched off the hybridization of the 4f states with all other valence states and treated the R 4f states in the spherical part of the crystal potential as the atomic-like core states. The hybridization shift of the CF levels was estimated in the case of cubic Ce based NaCl-type compounds [19]. On the other hand, hexagonal RAl_3 compounds with more than one localized 4f electron provide a complicated case for this kind of theory starting from the Anderson model and such a development is beyond the scope of the present paper. The integer numbers two and three were fixed for the occupation of the Pr 4f and Nd 4f states at the rare-earth lattice site, respectively. The CF parameters B_n^m originating from the aspherical part of the total single-particle DFT potential in the crystal can be obtained from

$$B_n^m \propto \int_0^\infty \left|\mathrm{R}_{4f}(r)\right|^2 V_n^m(r) r^2 \,\mathrm{d}r \tag{3}$$

where the non-spherical component $V_n^m(r)$ also reflects, besides the nuclear potentials and Hartree part of the inter-electronic interaction, the exchange–correlation term, which accounts for many-particle effects [16]. The wavefunction R_{4f} describes the radial shape of the localized 4f charge density of the rare-earth ion in the studied compounds. It is well known that the use of a self-consistent LSDA or GGA 'open core' R_{4f} wavefunction leads to a poor description of the CF interaction, due to the so-called 'self-interaction' potential which is felt by the localized 4f electron and which is not correctly treated within the LSDA [17]. Therefore, the present study used the value of R_{4f} resulting from independent DFT calculations performed for the RAl_3 compounds using the optimized linear combination of atomic orbitals method (OLCAO) [17]. In the case of the OLCAO method the 4f states were treated using the self-interaction-corrected (SIC) DFT approach [18]. We note that equation (3) does not contain the type of exchange contribution to the CF parameters which was originally suggested by Chow [20]. This exchange contribution goes beyond the DFT methodology, which is based on a treatment of the single-particle crystal potential that is as reliable as possible. The change of the CF parameters with pressure is nevertheless expected to be roughly accounted for without this correction.

The CF parameters from our first principles DFT calculations are listed in table 3. The parameters have the same signs and the same order of magnitude as the best-fit parameters listed in table 1. The value of B_2^0 decreases from $PrAl_3$ to $NdAl_3$ by more than a factor of 2.5 compared to the analysis of the experimental data which give a decrease by a factor of 2.13. B_4^0 decreases by a factor of 10.5. The experimental B_4^0 also decreases when going from $PrAl_3$ to $NdAl_3$ but by a much smaller factor of 2.72. The absolute values of the experimental and the DFT parameters B_6^0 and B_6^6 both decrease when going from $PrAl_3$ to $NdAl_3$. These trends are well reproduced by our first principles calculations. To check further the quality of the DFT-based calculations we have diagonalized the microscopic CF Hamiltonian (equation (1)) using the calculated CF parameters from table 3. The resulting sequences and the spacings between the different CF levels are considerably different from what is found experimentally (figure 2). On the other hand, the total CF splitting of the ground-state multiplet of $PrAl_3$ and $NdAl_3$ is 16.9 and 15.2 meV, respectively, which again provides a reasonable estimation compared with the total CF splitting derived from the experiment (see figure 2). Therefore, we are able to capture the basic trends observed, in particular that the total strength of the CF interaction decreases when going from $PrAl_3$ to $NdAl_3$.

Next, we compare the calculated and experimental changes of the CF interaction under pressure in the case of $NdAl_3$ (see table 3). In our DFT calculations the density of states

at the Fermi level decreases under pressure and the occupied part of the valence band states is broadened as expected. It is to be noted that smaller changes of the CF parameters upon pressure have been found than were derived from the INS spectra. DFT calculations suggest that all absolute values of the CF parameters get bigger with the exception of B_2^0 which is almost the same, in contrast to the experiment which suggests an increase of B_2^0 of about 11%. It would be interesting to check the validity of the DFT-based approach upon pressures larger than several gigapascals in future experimental investigations. In our calculations, we have also found that the DFT-based CF parameters are rather sensitive to both the ground-state charge density distributions and the details of the shape of R_{4f}. The former fact is mainly connected with the values of the lattice parameters a and c and the value of the positional parameter x_{Al}. In all our calculations presented here, we therefore used the lattice geometry which follows from the experimental data. The latter fact points to the approximate treatment of the localized and highly correlated 4f states in state of the art DFT calculations. Moreover, we note that in the present DFT approach we have neglected any hybridization between the localized 4f states and the valence states in RAl_3. The hybridization shift of the CF levels in our opinion can also contribute to the origin of CF interaction in the light RAl_3 compounds, i.e. particularly in $PrAl_3$.

5. Conclusions

INS measurements of the paramagnetic CF splittings of $PrAl_3$ and $NdAl_3$ have been carried out. Compared to earlier CF studies on $PrAl_3$, the present data now allow for a non-ambiguous parametrization of the CF. The CF of $NdAl_3$ has been measured at ambient pressure and at $p = 0.84$ GPa. Pressure is found to shift the CF levels to higher energies without any principal new features occurring in the CF splitting. The substantial shifts in the CF were discussed within the extended PCM as well as by DFT calculations. The latter can reproduce the signs and the orders of magnitude of the experimentally determined CF parameters as well as the magnitude of the CF splitting at ambient pressure and at pressures below 1 GPa. This suggests that the methodology based on the DFT calculations of the ground-state charge density can be used to obtain the starting values of CF parameters for rare-earth intermetallics which can be further refined using the analysis of INS data. Both the DFT calculations and the extended PCM underestimate the effect of pressure.

Acknowledgments

This work was performed at the Swiss Spallation Neutron Source SINQ, Paul Scherrer Institut (PSI), Villigen, Switzerland. We are indebted to Peter Allenspach, Thomas Mühlebach and Rudolf Thut for help with the magnetic measurements under pressure. Two authors (MD and JR) acknowledge fruitful discussions with Bernard Delley, Manuel Richter, Peter Blaha, Helmut Eschrig and Karlheinz Schwarz as well as financial support by the Grant Agency of the Czech Republic (grants 202/03/0552 and 202/02/0739), the Grant Agency of Charles University (grant 145/2000/B) and the research programme MSM113200002.

References

[1] Alekseev P A, Sadikov I P, Markova I A, Savitskii E M, Terekhova V F and Chistyakov O D 1976 *Sov. Phys.–Solid State* **18** 389

[2] Alekseev P A, Shitikov Yu L, Markova I A, Chistyakov O D, Savitskii E M and Kjems J 1982 *Phys. Status Solidi* **114** 161

[3] Andreef A, Kaun L P, Lippold B, Matz W, Moreva N I and Walther K 1978 *Phys. Status Solidi* **87** 535
[4] Goossens D J, Kennedy S J and Hicks T J 1998 *Physica* B **241–243** 654
[5] Alekseev P A, Goremychkin E A, Lippold B, Mühle E and Sadikov I P 1983 *Phys. Status Solidi* **119** 651
[6] Mahoney J V, Wallace W E, Craig R S and Sankar S G 1975 *Inorg. Chem.* **14** 2918
[7] Skelton E F, Webb A W, Qadri S B, Wolf S A, Lacoe R C, Feldman J L, Elam W T, Carpenter E R Jr and Huang C Y 1984 *Rev. Sci. Instrum.* **55** 849
[8] Villars P and Calvert L D 1991 *Pearson's Handbook of Crystallographic Data for Intermetallic Phases* (Materials Park, OH: Material Information Society)
[9] Bireckoven B and Wittig J 1988 *J. Phys. E: Sci. Instrum.* **21** 841
[10] Morrison C A 1988 *Angular Momentum Theory Applied to Interactions in Solids* (Berlin: Springer)
[11] Freeman A J and Desclaux J P 1979 *J. Magn. Magn. Mater.* **12** 11
[12] Strässle Th, Altorfer F and Furrer A 2001 *J. Phys.: Condens. Matter* **13** 6773
[13] Walter U 1984 *J. Phys. C: Solid State Phys.* **45** 401
[14] Blaha P, Schwarz K and Luitz J 1997 *WIEN97, a Full Potential Linearized Augmented Plane Wave Package for Calculating Crystal Properties* Technical University of Vienna (ISBN 3-9501031-0-4)
This is an improved and updated Unix version of the original copyrighted WIEN code, which was published by Blaha P, Schwarz K, Sorantin P and Trickey S B 1990 *Comput. Phys. Commun.* **59** 399
[15] Perdew J P, Burke S and Ernzerhof M 1996 *Phys. Rev. Lett.* **77** 3865
[16] Diviš M, Rusz J, Hilscher G, Michor H, Blaha P and Schwarz K 2002 *Czech. J. Phys.* **52** 283
[17] Richter M 1998 *J. Phys. D: Appl. Phys.* **31** 1017
[18] Diviš M, Richter M, Forstreuter J, Koepernik K and Eschrig H 1997 *J. Magn. Magn. Mater.* **176** L81
[19] Wills J M and Cooper B R 1987 *Phys. Rev.* B **36** 3809
[20] Chow H C 1973 *Phys. Rev.* B **7** 3404